

Low-Magnetic-Field Divergence of the Electronic g Factor Obtained from the Cyclotron Spin-Flip Mode of the $\nu = 1$ Quantum Hall Ferromagnet

A. B. Van'kov,^{1,2} L. V. Kulik,^{1,2} I. V. Kukushkin,^{1,2} V. E. Kirpichev,^{1,2} S. Dickmann,¹ V. M. Zhilin,¹ J. H. Smet,² K. von Klitzing,² and W. Wegscheider^{3,4}

¹*Institute for Solid State Physics, Russian Academy of Sciences, Chernogolovka 142432, Russia*

²*Max-Planck-Institut für Festkörperforschung, Heisenbergstraße 1, 70569 Stuttgart, Germany*

³*Walter Schottky Institut, Technische Universität München, 85748 Garching, Germany*

⁴*Institut für Experimentelle und Angewandte Physik, Universität Regensburg, 93040 Regensburg, Germany*

(Received 30 May 2006; published 11 December 2006)

We report an inelastic light scattering study of the cyclotron spin-flip mode in the two-dimensional electron system at filling $\nu = 1$. The energy of this mode can serve as a probe of the many-body exchange interaction on short length scales. Its magnetic field dependence is compared with predictions based on Hartree-Fock theory. They agree well when including the nonzero width of the electron system. From the measured energies, the exchange enhanced g factor is extracted. It diverges at small fields and differs largely from g factors obtained via transport activation studies.

DOI: [10.1103/PhysRevLett.97.246801](https://doi.org/10.1103/PhysRevLett.97.246801)

PACS numbers: 73.43.Lp, 71.70.Ej, 75.30.Ds

The recent focus on making use of the spin degree of freedom has also revived an interest in basic studies of the enhanced g factor and itinerant ferromagnetism at, for instance, filling $\nu = 1$ in GaAs/AlGaAs and Si/SiGe two-dimensional heterostructures ($\nu = n/N_\phi$, where n is the electron density and N_ϕ is the orbital degeneracy per unit area of a Landau level) [1–6]. For weak Zeeman coupling, the $\nu = 1$ ground state is nondegenerate with the total spin quantum number $S = N_\phi/2$ and the spin projection along the magnetic field axis $S_z = N_\phi/2$. The simplest neutral excitations referred to as spin excitons have a single reversed spin. Their nature changes from having collective spin-wave character in the long wave limit $ql_B \rightarrow 0$ to having single particle character in the opposite limit $ql_B \rightarrow \infty$. Here, q is the 2D momentum, and l_B is the magnetic length. A spin exciton in the limit $ql_B \rightarrow \infty$ is composed of an excited electron in the empty spin branch of the Landau level and the hole left behind at a large spatial separation in the filled branch of the Landau level with opposite spin [7]. The energy to form such a pair at zero temperature is the exchange enhanced spin splitting. It is written as $g_{\text{eff}}(B)\mu_B B$, where $g_{\text{eff}}(B)$ is the enhanced or effective g factor and μ_B is the Bohr magneton, and can be obtained from temperature dependent transport experiments.

From such a collection of transport studies [1–4], we conclude that this splitting at fixed filling $\nu = 1$ increases in essence linearly with B ; i.e., g_{eff} remains more or less constant. This observation contradicts simulations within the Hartree-Fock (HF) framework. They predict that the exchange enhanced spin splitting is proportional to \sqrt{B} [7,8]. Some attempts have been made to extend the theory. In one instance, dynamical screening of the exchange interaction was incorporated within the random phase approximation (RPA) [9]. The screening correction was found to be important below 1 T. At larger fields though,

the RPA contribution is fairly small. Spin texture excitations, referred to as finite-size Skyrmions and carrying one unit of (topological) charge, have also been considered [10]. The Skyrmion approach has been successful in elucidating some nuclear resonance [11], optical absorption [12], and transport experiments [2]. However, it does not provide an explanation for other transport [1,3–6] and luminescence data [13]. All the aforementioned experimental techniques deal with averaged, macroscopic characteristics of the 2D electron system, which apart from Coulomb interaction are likely also influenced by poorly controlled perturbations such as, for instance, the disorder potential. In general, it would be highly desirable to obtain experimental data on the exchange interaction with a method for which the outcome is not affected by disorder or fluctuations on length scales exceeding the magnetic length but for which only the interparticle scale matters.

It turns out that the energy of the cyclotron spin-flip mode—an excitation which as opposed to a spin exciton involves a concurrent change of the orbital and spin quantum numbers—measured with inelastic light scattering may just provide this information about the exchange interaction even when measuring at small wave numbers [14]. For other excitations such as magnetoplasmons and spin excitons, the exchange interaction contributes only at large momenta, difficult to access in experiment, as a result of the Kohn and Larmor theorems [15,16]: homogenous electromagnetic radiation incident on a translationally invariant electron system is unable to excite internal degrees of freedom associated with the Coulomb interaction, and in a system with rotational invariance in spin space Coulomb interaction does not contribute to the energy of zero-momentum spin excitons. Such arguments, however, do not apply to the zero-momentum cyclotron spin-flip mode (CSFM). Both theory and experiment have established that this mode excited from spin-polarized ground states ac-

quires considerable exchange energy even for $q \rightarrow 0$ [8,14,17,18]. Moreover, the CSFM is dispersionless, i.e., its energy is basically constant, up to wave number $q \sim 1/l_B$ [14,17]. Hence, a violation of translation symmetry on distances larger than the magnetic length (due to disorder for instance) does not disturb the CSFM energy. This mode may thus be regarded as a unique *local* probe of many-body interactions. It has already proven valuable for understanding the physics of neutral excitations of some quantum Hall states [19–22]. Here, its properties are exploited to test how well Hartree-Fock theory performs over a large magnetic field span as well as to obtain the exchange enhanced g_{eff} as a function of B . These measurements shed new light on the behavior of g_{eff} as they reveal a dramatic difference with values acquired from activated transport experiments.

Our studies were carried out on single sided doped $\text{Al}_{0.33}\text{Ga}_{0.67}\text{As}/\text{GaAs}$ quantum wells (QWs) with a QW width of 20, 25, and 30 nm. The mobility varied between 2 and $7 \times 10^6 \text{ cm}^2/\text{Vs}$ and the density n ranged from 1 to $2.5 \times 10^{11} \text{ cm}^{-2}$. The latter was changed using the optodepletion effect and measured by means of photoluminescence [23]. The experiments were performed at 0.3 K. The optical measurements were carried out with a multiple glass fiber arrangement [18]. One fiber transmitted a Ti:sapphire laser beam tuned above the fundamental band gap in GaAs in order to excite the electronic system at a power density below $0.1 \text{ W}/\text{cm}^2$. The scattered light was collected with another fiber. The angles between the sample surface and the fibers responsible for pumping and collecting defined the transferred momentum. By having multiple collecting fibers at different angles, it was possible to change *in situ* the transferred momentum. The scattered light was dispersed in a T-64000 triple spectrograph and recorded with a CCD camera.

Figure 1(a) shows typical Raman spectra at filling $\nu = 1$. They exhibit four lines. Two of them correspond to collective excitations: the hybrid magnetoplasma (MP) and the cyclotron spin-flip mode [18]. The MP energy at $q|_B \rightarrow 0$ may be estimated from the RPA formula [24]

$$\hbar \omega_{\text{MP}}(q) \approx \sqrt{(\hbar \omega_c)^2 + (\hbar \omega_p)^2}. \quad (1)$$

Here, $\omega_p = (ne^2q/2\epsilon\epsilon_0m_e^*)^{1/2}$ is the plasma frequency, and $\omega_c = eB/m^*$ is the cyclotron frequency. The cyclotron-spin-flip energy can be written as

$$E_{\text{CSFM}}(q) = \hbar \omega_c + |g^* \mu_B B| + \Delta(q, B). \quad (2)$$

It is composed of three contributions: the cyclotron gap, the bulk Zeeman energy $g^* \mu_B B$ ($g^* = -0.44$), and a Coulomb term $\Delta(q, B)$ equal to the difference between the interaction energy of the ground state and the excited state with one spin flipped [14,17]. The bulk Zeeman term at the experimental conditions in Fig. 1 is only 0.16 meV and negligible compared to the other terms. The observed Coulomb term is large [inset of Fig. 1(a)] and hence it can be measured with high precision. Little is known about

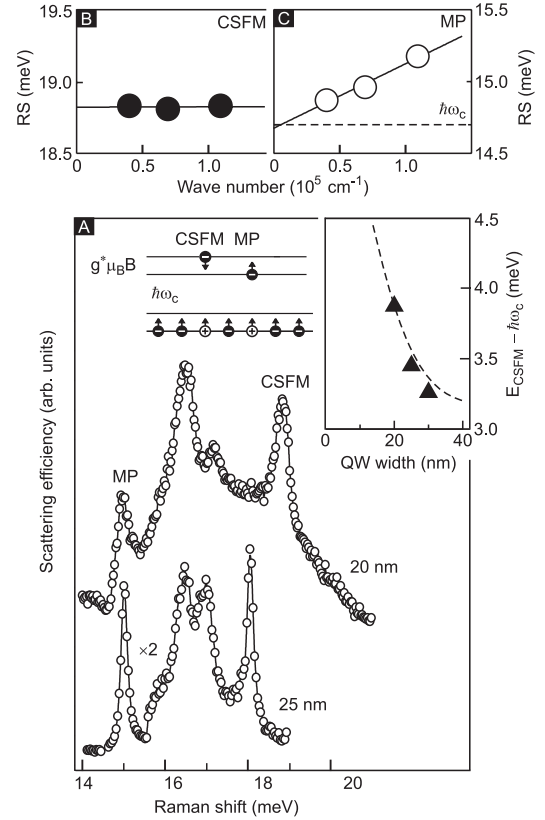


FIG. 1. (a) Raman spectra at 8.5 T ($\nu = 1$) for a 20 and 25 nm QW. The inset compares $\Delta(0, B = 7.6 \text{ T})$ extracted from experiment for three QWs (solid triangles) with a Hartree-Fock simulation (dashed line). The upper graphs display the dispersion of the Raman shift (RS) in the long wavelength limit for the CSFM (b) and the MP mode (c).

the nature of the remaining spectral features in Fig. 1(a). In Ref. [14], they are attributed to inelastic light scattering from the MP mode with momenta corresponding to extremal points in the dispersion. Such scattering might be possible, if wave vector conservation no longer strictly holds due to short scale residual disorder.

At the experimentally accessible momenta, the MP dispersion behaves linearly [Fig. 1(c)]. The CSFM energy, however, shows no change with wave number [Fig. 1(b)]. Hence, one can replace $\Delta(q, B)$ in Eq. (2) with $\Delta(0, B)$ for the q values accessible in experiment. Figure 1 illustrates how the CSFM energy enhances in narrower QWs. The increase in $\Delta(0, B)$ with decreasing QW width originates from reduced Coulomb softening as the width of the wave function in the growth direction shrinks. To properly account for this nonzero thickness effect, the Fourier components of the Coulomb potential $v(q) = e^2/2\epsilon\epsilon_0q$ should be multiplied with a geometrical form factor $F(q)$: $\bar{v}(q) = v(q)F(q)$. The form factor is given by

$$F(q) \approx \int_0^\infty dz \int_0^\infty dz' |\psi(z)|^2 |\psi(z')|^2 e^{-q|z-z'|}, \quad (3)$$

where $\psi(z)$ is the wave function in the growth direction. The form factor monotonically decreases with q to reflect

that the effective Coulomb potential $\bar{v}(r) = \int d^2q e^{i\mathbf{q}\cdot\mathbf{r}} \bar{v}(q)/4\pi^2$ falls off slower than it would for a $1/r$ behavior. Note that the form factor is itself independent of B . The dependence of $\Delta(0, B)$ on B enters through the magnetic length l_B . It selects the range of q values that contribute to the interaction energies [see Eqs. (4) and (5) below]. In small B fields when $l/l_B \ll 1$ (l is the full width at half maximum of the wave function) the Coulomb interaction is effectively 2D and scales with \sqrt{B} . In the opposite limit at high fields where $l/l_B \gg 1$ electrons can be thought of as long charged rods interacting via Coulomb forces and the Coulomb interaction softens. The interaction energy then exhibits a weak logarithmic B dependence instead. In the experiment of Fig. 2, indeed $\Delta(0, B)$ increases slower than \sqrt{B} at high fields. A transition between both limits occurs in the range of fields studied: $l/l_B \approx 2$ at 9 T.

In Fig. 2 the experimental values for $\Delta(0, B)$ are compared with HF simulations as in Refs. [7,8], but with the

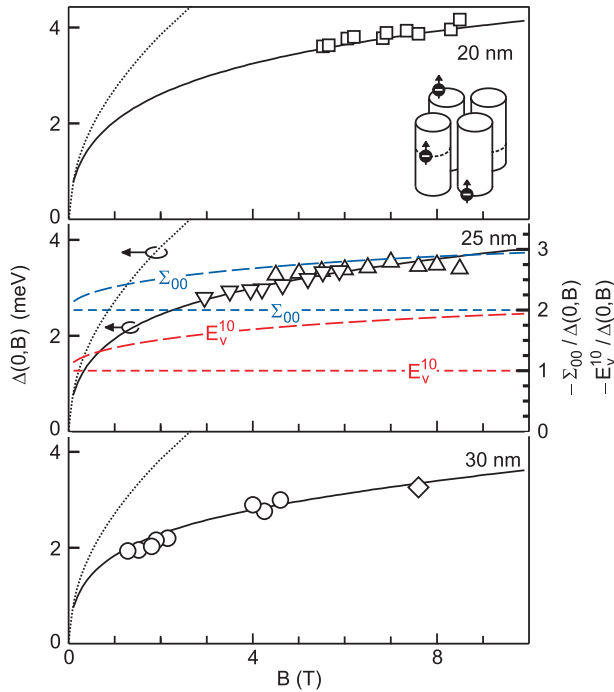


FIG. 2 (color). $\Delta(0, B)$ values extracted from Raman experiments for QWs with different widths (open symbols) in comparison with Hartree-Fock simulations, which take into account the nonzero width of the wave function via form factor $F(q)$ (solid lines). Dotted lines show the \sqrt{B} behavior predicted by Hartree-Fock for the strict 2D case, i.e., when $F(q) = 1$. Different symbols correspond to different heterostructures used for collecting the data. The form factor is calculated from the wave function, which itself is obtained from a self-consistent solution of the Schrödinger and Poisson equations. The inset pictorially explains the softening of the Coulomb interaction with B when the FWHM of the wave function l exceeds l_B . The middle panel shows on the right axis $-\Sigma_{00}/\Delta(0, B)$ (blue curves) and $-E_v^{10}/\Delta(0, B)$ (red curves) for a 25 nm QW (long-dashed curve) and the strict 2D case (short-dashed curve).

inclusion of the geometrical form factor. When the CSFM is excited the electron system loses the electron exchange self-energy $\Sigma_{00}(B)$ of the 0th Landau level,

$$\Sigma_{00}(B) = - \int \frac{d^2k}{(2\pi)^2} \bar{v}(k) e^{-k^2 l_B^2/2}, \quad (4)$$

as there exists no exchange interaction between the electrons in different spin states. This energy loss is partly compensated by the exciton binding energy

$$E_v^{10}(0, B) = - \int \frac{d^2k}{(2\pi)^2} \bar{v}(k) \left[1 - \frac{k^2 l_B^2}{2} \right] e^{-k^2 l_B^2/2}, \quad (5)$$

between the excited electron in the first Landau level and the hole left behind in the zeroth Landau level (vertex corrections). Because of different orbital quantum numbers, the electron and hole form a “ p ” exciton [25]. These two terms contribute to $\Delta(0, B)$ [14,26]:

$$\Delta(0, B) = -\Sigma_{00}(B) + E_v^{10}(0, B). \quad (6)$$

The solid lines in Fig. 2 show the theoretical result. The agreement with the experiment is noteworthy, but only if finite thickness is taken into account. The dotted lines are obtained for the strict 2D case and are far off. In Fig. 3(a) the same experimental data for the different QW widths W are replotted but the values are normalized by dividing with the theoretical ratio $\Delta_W(0, B)/\Delta_{25 \text{ nm}}(0, B)$ (the subscript denotes the QW width).

The exchange self-energy $\Sigma_{00}(B)$ is related to the exchange enhanced spin splitting observed in magnetotransport experiments [1–6] according to $|g_{\text{eff}} \mu_B B| = |g^* \mu_B B| - \Sigma_{00}(B)$. In the strict 2D case, i.e., when $F(q) = 1$, $|\Sigma_{00}|/\Delta(0, B) = 2$ for any field [14]. The influence of finite width alters this ratio from 2 at $B = 0$ to 3 at high field as shown for the 25 nm QW in Fig. 2. The excellent

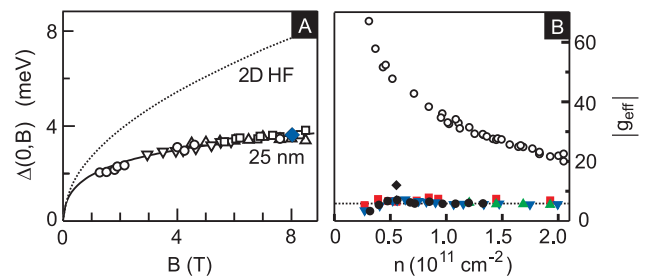


FIG. 3 (color). (a) Normalized values of $\Delta(0, B)$ (same symbols as in Fig. 2) for the 20, 25, and 30 nm QWs. The normalization coefficient is equal to the ratio of $\Delta(0, B)$ for a QW of width W predicted by theory to the theoretical value of $\Delta(0, B)$ for a 25 nm QW. The solid line is the Hartree-Fock result for the 25 nm QW. The previously reported data point from Ref. [14] is also displayed as a blue diamond. (b) The exchange enhanced g_{eff} versus density (or equivalently B) calculated from the experimental data points as described in the text. Previously reported data from transport activation experiments are also shown: red squares [1], black diamonds [2], green (up-pointing) triangles [3], and blue (down-pointing) triangles [4].

agreement of the $\Delta(0, B)$ values with theory warrant the extraction of g_{eff} from the data using the calculated ratio $|\Sigma_{00}|/\Delta(0, B)$. The results are plotted in Fig. 3(b) and compared with previously reported values of g_{eff} from magnetotransport [1–4]. The two sets of data differ largely. At low B the exchange enhanced g_{eff} acquired via Raman scattering exceeds the transport data by an order of magnitude. It reaches values as high as 60 and seems to diverge in the $B \rightarrow 0$ limit as expected from a dimensional analysis. The activation data, on the other hand, coalesce onto a horizontal line, which describes a B -independent $|g_{\text{eff}}|$ of approximately 6. A previously reported Raman data point [14] as well as a data point obtained with a different method [28] agree with our results. The divergence is in line with the predicted Stoner instability [29] for dilute 2D electron systems at $B = 0$ [28,30–32], although our experimental arrangement is unable to prove this instability.

We conjecture that this large discrepancy between the Raman and transport results originates from the different susceptibility to the disorder potential of the quantities measured in these experiments. As a consequence of random potential fluctuations, electrons of the lowest Landau level experience on average a weaker exchange field than the HF field and the activation energy and hence the g factor extracted from activation studies is significantly reduced. In fact, although the sample mobility may not be the best measure of the random potential fluctuations, indeed the activation gap is systematically smaller in lower mobility samples [1]. In Raman scattering, however, the signal stems from those parts of the sample where the CSFM exists, i.e., where translation symmetry is not violated on the scale of the interparticle distance. Hence, by looking at the CSFM, only those areas in the sample with ferromagnetic ordering are selected. In those regions the exchange energy reaches its maximum HF value. This self-selection mechanism is absent in macroscopic transport studies. Scattering from regions with no ferromagnetic order might be responsible for the background signal, spanning from the MP energy to the CSFM energy (Fig. 1). This interpretation is strengthened by the observation of an enhanced background in samples with lower mobility.

In conclusion, we have investigated the magnetic field dependence of the cyclotron spin-flip mode energy of the $\nu = 1$ quantum Hall ferromagnet using inelastic light scattering. Exchange interaction energies extracted from these measurements agree well with a Hartree-Fock simulation provided that the finite width of the 2D system is taken into account. In the high field limit, the nonzero width turns the Coulomb interaction energy nearly independent of the magnetic field. In the low field limit the observed energies suggest a divergence of the effective electron g factor as one would expect from theory, but in disagreement with activated transport studies. A measurement of the CSFM energy seems to avoid the influence of the disorder potential, which apparently averages and results in the drastically reduced g values deduced from transport studies.

We acknowledge support from the BMBF, the CRDF, the INTAS, the DFG, and the RFBR.

-
- [1] A. Usher, R. J. Nicholas, J. J. Harris, and C. T. Foxon, *Phys. Rev. B* **41**, 1129 (1990).
 - [2] A. Schmeller, J. P. Eisenstein, L. N. Pfeiffer, and K. W. West, *Phys. Rev. Lett.* **75**, 4290 (1995).
 - [3] V. T. Dolgoplov *et al.*, *Phys. Rev. Lett.* **79**, 729 (1997).
 - [4] V. S. Khrapai *et al.*, *Phys. Rev. B* **72**, 035344 (2005).
 - [5] V. S. Khrapai, A. A. Shashkin, and V. T. Dolgoplov, *Phys. Rev. B* **67**, 113305 (2003).
 - [6] M. A. Wilde *et al.*, *Phys. Rev. B* **72**, 165429 (2005).
 - [7] Yu. A. Bychkov, S. V. Iordanskii, and G. M. Eliashberg, *Pis'ma Zh. Eksp. Teor. Fiz.* **33**, 152 (1981) [*JETP Lett.* **33**, 143 (1981)].
 - [8] C. Kallin and B. I. Halperin, *Phys. Rev. B* **30**, 5655 (1984).
 - [9] A. P. Smith, A. H. MacDonald, and G. Gumbs, *Phys. Rev. B* **45**, 8829 (1992).
 - [10] S. L. Sondhi, A. Karlhede, S. A. Kivelson, and E. H. Rezayi, *Phys. Rev. B* **47**, 16419 (1993).
 - [11] S. E. Barrett *et al.*, *Phys. Rev. Lett.* **74**, 5112 (1995).
 - [12] M. J. Manfra *et al.*, *Phys. Rev. B* **54**, R17327 (1996).
 - [13] I. V. Kukushkin, K. von Klitzing, and K. Eberl, *Phys. Rev. B* **55**, 10607 (1997); **60**, 2554 (1999).
 - [14] A. Pinczuk *et al.*, *Phys. Rev. Lett.* **68**, 3623 (1992).
 - [15] W. Kohn, *Phys. Rev.* **123**, 1242 (1961).
 - [16] M. Dobers, K. von Klitzing, and G. Weimann, *Phys. Rev. B* **38**, 5453 (1988).
 - [17] J. P. Longo and C. Kallin, *Phys. Rev. B* **47**, 4429 (1993).
 - [18] L. V. Kulik *et al.*, *Phys. Rev. B* **63**, 201402(R) (2001).
 - [19] M. A. Eriksson *et al.*, *Phys. Rev. Lett.* **82**, 2163 (1999).
 - [20] L. V. Kulik *et al.*, *Physica (Amsterdam)* **12E**, 574 (2002).
 - [21] L. V. Kulik *et al.*, *Phys. Rev. B* **72**, 073304 (2005).
 - [22] S. Dickmann and I. V. Kukushkin, *Phys. Rev. B* **71**, 241310(R) (2005).
 - [23] I. V. Kukushkin and V. B. Timofeev, *Adv. Phys.* **45**, 147 (1996).
 - [24] K. W. Chiu and J. J. Quinn, *Phys. Rev. B* **9**, 4724 (1974).
 - [25] I. V. Lerner and Yu. E. Lozovik, *Zh. Eksp. Teor. Fiz.* **78**, 1167 (1980) [*Sov. Phys. JETP* **51**, 588 (1980)].
 - [26] Equation (5) is not entirely correct even when considering only first order interaction terms [22,27]. The CSFM hybridizes with a two-exciton state formed out of the $\delta S = -1$, $\delta n = 0$ spin wave and the $\delta S = 0$, $\delta n = 1$ magnetoplasmon with opposite momenta (δS and δn are the change in the spin and orbital quantum numbers). Hence, the CSFM is really a four-particle excitation. This is taken into account in the excitonic representation [22,27]. Here we restrict ourselves to the standard HF approach. It lends itself for the inclusion of finite thickness, which is the key ingredient to obtain good agreement between experiment and theory.
 - [27] S. Dickmann, V. M. Zhilin, and D. V. Kulakovskii, *JETP* **101**, 892 (2005).
 - [28] B. A. Piot *et al.*, *Phys. Rev. B* **72**, 245325 (2005).
 - [29] E. C. Stoner, *Rep. Prog. Phys.* **11**, 43 (1947).
 - [30] C. Attacalite *et al.*, *Phys. Rev. Lett.* **88**, 256601 (2002).
 - [31] J. Zhu *et al.*, *Phys. Rev. Lett.* **90**, 056805 (2003).
 - [32] Y. Zhang and S. Das Sarma, *Phys. Rev. B* **72**, 115317 (2005).